An Impedance Matrix Transformation for Planar Circuit Integral Equation Solvers

F. Cervelli, M. Mongiardo, L. Tarricone

Istituto di Elettronica
Via G. Duranti, 93, 06131, Perugia, Italy.

Abstract— **We describe an efficient analysis of planar circuits which makes use of a state-of-the-art integral equation approach in conjunction with a new bandwidth reduction algorithm.**
The MPIE is formulated by considering the recently introduced closed form expressions for the Green's functions; standard roof-top basis functions are used during the discretization of the Method of Moments. The matrix sparseness introduced by a thresholding procedure has proven sufficient for the application of an effective bandwidth reduction algorithm which yields, in all the considered cases, a significant reduction of computer effort (maximum speed-ups of about 18 times).

I. Introduction

Efficient modeling of printed circuits and antennas is crucial in current microwave engineering [1], [2] and has stimulated several contributions: in particular a mixed-potential integral equation (MPIE) was proposed by Mosig [3], [4] and, more recently, the latter formulation was enhanced by the evaluation of suitable closed-form spatial-domain Green's functions [5]. Considerable efforts are currently made to improve the efficiency and accuracy of these numerical methods, e.g. the inclusion of 3D unknown currents; efficient choices for the Sommerfeld integration paths [6]; the enhancement of the complex-image method [7] for multilevel stratified microstrip lines [8], [9]. The above mentioned contributions are mainly in the direction of reducing the computation time required for filling the impedance matrix.

Another direction of investigation has been to consider a basis function expansion such as to improve matrix sparseness [10], [11] by using wavelets. However, their introduction requires significant changes in the theoretical formulation of the problem and in the code implementation, hence preventing their wide application.

We present a different approach, which allows us to obtain sparse matrices (via an appropriate *thresholding* of its elements) with banded structure, by suitably *renumbering* standard type of basis functions. This approach is particularly appealing since it can be employed with minimal, if any, change in the code structure; moreover the relative performances are substantially superior to other previous approaches.

The paper is structured as follows: Section 2 describes the main features of the MPIE approach with closed-form Green's functions, while Section 3 focusses on its numerical properties. Section 4 describes the strategy to improve performances via the renumbering algorithm. Section 5 presents some results, and finally conclusions are drawn.

II. The MPIE approach with Closed-form Green's Functions

The MPIE is obtained by using Leontovich boundary condition, after suitable selections of the vector potential $\mathbf{A}$, of the Lorentz Gauge, and by introducing the Green's functions $\bar{\bar{\mathbf{G}}}^{\mathbf{A}}$ and G^q for the surface electric current density $\mathbf{J_S}$ and for the surface electric charge density q_S. In this way, the following MPIE equation is recovered:

$$\mathbf{n}\times\mathbf{E^e}(\mathbf{r}) = \mathbf{n}\times(\mathbf{Z_S}\mathbf{J_S} - \mathbf{j}\omega\int_{\mathbf{S}}\bar{\bar{\mathbf{G}}}^{\mathbf{A}}\cdot\mathbf{J_S}\,\mathbf{dS'} + \nabla\int_S G^q\cdot q_S\,dS') \tag{1}$$

In the (1), $\mathbf{E^e}$ denotes the excitation electric field, and $\mathbf{Z_s}$ and $\mathbf{J_S}$ denote the surface impedance and electric current density respectively. As initially proposed for single-layer structures, [7], and furtherly extended to multi-layer problems, [12], [13], [14], closed-form spatial domain Green's functions can be analytically evaluated.

The equation (1) is discretized and solved using the Galerkin's version of MoM, together with roof-top basis functions, so that a linear system

$$\begin{bmatrix} Z_{xx} & Z_{xy} \\ Z_{yx} & Z_{yy} \end{bmatrix}\begin{bmatrix} I_x \\ Iy \end{bmatrix} = \begin{bmatrix} V_x \\ Vy \end{bmatrix} \tag{2}$$

is generated. The entries Z_{ij} in the impedance matrix represent the tangential electric field generated by the j-th basis function and weighted by the i-th test one.

III. Numerical Properties of the Linear System

The accuracy of the implemented method is demonstrated in Fig. 1, where numerical results are compared with experimental data for a double stub [15]. As apparent from this figure, the theoretical amplitude and phase are both in good accordance with experimental data.

A significant amount of the numerical effort of the above problem is in the solution of the linear system (2). It can be performed using a standard dense Gaussian solver, as the system matrix is generally dense. A more detailed analysis on real cases, anyway, opens different perspectives. In Fig. 2,3 the patterns of the system matrix for the two circuits reported in the respective figures are shown. Different gray levels correspond to different magnitudes (white is zero, black is the maximum magnitude in the matrix). A value smaller than 10^{-9} is zeroed. It can be easily noted that several entries can be neglected. It is apparent that, even using standard roof-top basis functions, only a few entries retain an amount of information significant enough to solve the problem with adequate accuracy. Therefore, it makes sense to ask the following question: *how is the numerical accuracy affected when all entries smaller than a certain threshold value, v_t, are neglected?*. We include in Fig. 2,3 a table providing some clues to answer this question. For several values of v_t, the system solution and the circuit scattering parameters are evaluated and compared with the values computed considering all the entries in the system matrix. This way, an extimation of the errors due to the thresholding performed on the matrix entries is feasible. It can be observed that for values of v_t smaller than $10^{-5} \cdot z_{max}$ (where z_{max} is the maximum entry in the matrix), numerical errors are still comparable with experimental ones. This observation is also confirmed on several other test circuits.

On the basis of this consideration, it can be concluded that in many cases the system matrix can be reduced to a significantly sparse one without affecting the numerical accuracy. Its percentage of non-zero entries (we call it *sparsity*) depends on v_t. When a circuit must be modeled in a certain frequency range, the matrix sparsity can be preserved at every frequency, if the appropriate v_t is evaluated at the maximum frequency value.

IV. Speeding-up the System Solution

As the system (2) can be considered sparse, a first and trivial speed-up can be achieved by using a sparse solver, such as, for instance, an iterative biconjugate gradient method (BCG). Luckily, as demonstrated in [16], in several electromagnetic (EM) numerical problems, an alternative strategy can be quite effective. It consists in performing a suitable transformation on the system matrix, so that it is transformed into a banded one with reduced bandwidth; thereafter banded solvers can be used with very high performance. In fact, the solution time depends quadratically on the matrix bandwidth, and the effect of an effective bandwidth reduction is considerable.

In this paper, a new method, called Wonderful Bandwidth Reduction Algorithm (WBRA), is used to perform bandwidth reduction, superior to previous commercial and public-domain ones. It is developed in order to achieve high effectiveness on the typical patterns of sparse matrices encountered in EM numerical problems. Since it is described in [17], the interested reader is addressed to this reference for further details.

Therefore, the proposed strategy can be summarized in the following steps

- Verify if a suitable v_t exists and select it
- Set to zero all the matrix entries smaller than v_t
- Transform with WBRA the sparse linear system into a banded linear system
- Use a banded solver to solve the system

V. Results

In this section we compare the performance of the MPIE/MoM implementation with a standard dense Gaussian (DG) algorithm used to solve the linear system (2), with respect to using the BCG sparse one or the WBRA together with a banded LU direct solver (BN). The DG, the BCG and the banded solver are available in LAPACK public domain library.

The first example is the 2-port circuit of Fig. 2. For this circuit, studied in the range 2.5-3.5 GHz, the relative dielectric constant is 2.6, and the cell dimension is 3 mm (squared cells are considered). The system matrix has a size of 220, and after using $v_t = 10^{-5}$, it becomes a matrix with a sparsity of around 73%, and bandwidth 208. After using WBRA (which execution takes around 0.5 s) the final bandwidth of the transformed matrix is 72. In Tab. I, the time to evaluate a dispersion curve with 100 frequency-points is given for the three implementations (DG, BCG and WBRA+BN). Times are in seconds, and refer to an IBM 250 T.

Method	*Total Time*
GJ	6200
BCG	1832
$WBRA+BN$	1243

Table I

The second example is the 4-port branch coupler of Fig. 3. For this circuit, studied in the range 2.5-3.5 GHz, the relative dielectric constant is 2.6, and the cell dimension is 3 mm (squared cells are considered). The system matrix has a size of 401, and after using $v_t = 10^{-5}$, it becomes a matrix with a sparsity of around 81%, and bandwidth 310. After using WBRA (which execution takes around 2 s) the final bandwidth of the transformed matrix is 82. In Tab. II, the time to evaluate a dispersion curve with 100 frequency-points is given for the three implementations (DG, BCG and WBRA+BN). Times are in seconds, and refer to an IBM 250 T.

Method	*Total Time*
GJ	33860
BCG	4497
$WBRA+BN$	1835

Table II

As proved by the presented results, the use of a thresholding on matrix entries, coupled with a transformation of the same so that the bandwidth is reduced and a banded solver can be used with high efficiency, enhances

0-7803-4471-5/98/$10.00 (c) 1998 IEEE

meaningfully the package performance (5 times for the 2-port circuit, 18 times for the 4-port one). It is also superior to the use of iterative sparse solvers. The advantage of WBRA+BN strategy is increasingly evident for higher numbers of external ports of the circuit and for higher circuit complexity.

VI. Conclusion

In this paper a bandwidth reduction algorithm has been used in conjunction with an integral equation approach for the modeling of planar circuits. Based on a MPIE and using closed-form Green's functions, it ensures very high performance and noticeable accuracy, due to the exploitation of the numerical properties of the problem. In particular, by efficiently transforming the matrix of the linear system attained with the MoM, and using suitable system solvers, speed-ups of up to 18 times have been observed with respect to standard state-of-the-art implementations of the MPIE/MoM approach.

VII. Acknowledgment

Financial support from ASI (Italian Space Agency) and several discussions with Prof. R. Sorrentino are gratefully acknowledged.

References

[1] R. Sorrentino (Ed.), "Numerical Methods for Passive Microwave and Millimeter Wave Structures", *1989, IEEE Press, New York.*

[2] T. Rozzi and M. Mongiardo, "Open Electromagnetic Waveguides", *1997, IEE Press, London.*

[3] J. R. Mosig and F. E. Gardiol, "General integral equation formulation for microstrip antennas and scatterers", *Proc. Inst. Elec. Eng., pt. H: Microwave Optics Antennas*, vol. 132: pp. 424–432, Dec. 1985.

[4] J. R. Mosig, "Arbitrarly shaped microstrip structures and their analysis with a mixed potential integral equation", *IEEE Trans. Microwave Theory Tech.*, vol. 36: pp. 314–323, Feb. 1988.

[5] G. Dural and M. I. Aksun, "Closed-form Green's functions for general sources and stratified media", *IEEE Trans. Microwave Theory Tech.*, vol. 43: pp. 1545–1552, Jul. 1995.

[6] P. Gay-Balmaz and J. R. Mosig, "Three Dimensional Planar Radiating Structures in Stratified Media", *Int. J. MW and MM Wave Comp. Aided Eng.*, vol. 37: pp. 330–343, Sept. 1997.

[7] Y. L. Chow, J. J. Yang, D. G. Fang and G. E. Howard, "A closed-form spatial Green's function for thick microstrip substrate", *IEEE Trans. Microwave Theory Tech.*, vol. 39: pp. 588–592, Mar. 1991.

[8] C. H. Chan and R. A. Kipp, "Application of the Complex Image Method to the Multilevel, Multiconductor microstrip Lines", *Int. J. MW and MM Wave Comp. Aided Eng.*, vol. 37: pp. 359–367, Sept. 1997.

[9] C. H. Chan and R. A. Kipp, "Application of the Complex Image Method to the Characterization of Microstrip Vias", *Int. J. MW and MM Wave Comp. Aided Eng.*, vol. 37: pp. 368–379, Sept. 1997.

[10] K. F. Sabet, L.P.B. Katehi, K. Sarabandi, "Wavelet-based CAD Modeling of Microstrip Discontinuities using Least-Square Prony's Method", *IEEE MTT Int. Microwave Symp. Dig.*, pp. 1799–1802, 1997.

[11] K. F. Sabet, "Wavelet-based Modeling of Microstrip Circuits and Antennas", *IEEE MTT Workshop Dig.: Appl. of Wavelets to Electromagnetics*, 1996.

[12] M. I. Aksun and R. Mittra, "Derivation of closed-form Green's functions for a general microstrip geometry", *IEEE Trans. Microwave Theory Tech.*, vol. 40: pp. 2055–2062, Nov. 1992.

[13] I. Park, R. Mittra and M. I. Aksun, "Numerically efficient analysis of planar microstrip configurations using closed-form Green's functions", *IEEE Trans. Microwave Theory Tech.*, vol. 43: pp. 394–400, Feb. 1995.

[14] N. Kynaiman and M. I. Aksun, "Efficient and Accurate EM Simulation Technique for Analysis and Design of MMICs", *Int. J. MW and MM Wave Comp. Aided Eng.*, vol. 37: pp. 344–358, Sept. 1997.

[15] R. Jackson, "Full-Wave Finite Element Analysis of Irregular Microstrip Discontinuities" , *IEEE Trans. Microwave Theory Tech.*, vol. 37: pp. 81–89, Jan. 1989.

[16] M. Dionigi, A. Esposito, R. Sorrentino and L. Tarricone, "A Tabu Search Strategy for an Efficient Solution of Linear Systems in Electromagnetic Problems", *Int. Journal of Numerical Modelling*, vol. 10, 6, pp. 315-328, 1997.

[17] A. Esposito, S. Fiorenzo Catalano, F. Malucelli and L. Tarricone, "A new bandwidth matrix reduction algorithm", to appear in *Operations Research Letters*, 1998.

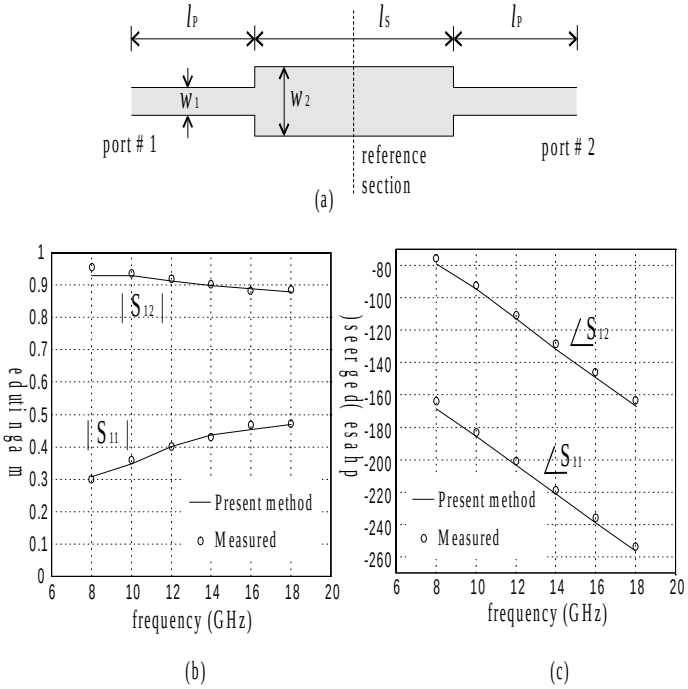

Fig. 1. Scattering parameters of matching section(a) in magnitude (b) and in phase (c). Physical dimensions: ε_r = 9.9, d = 10 mil,w_1 = 9.2 mil, w_2 = 23 mil, l_p = 30 mil, l_s = 50.6 mil

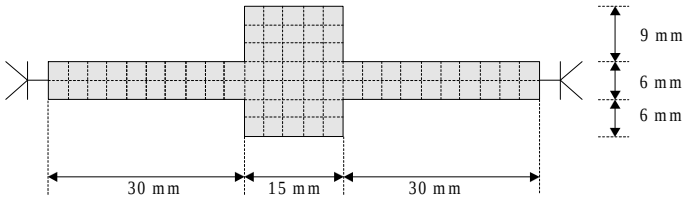

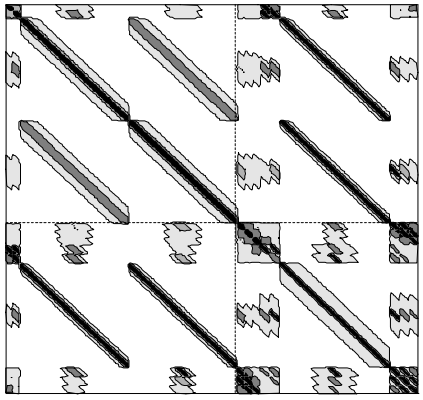

v_t	S	Solution Error	β Error	Scattering Parameter Error
10^{-7}	14.64 %	0.00 %	0.02 %	0.55 %
10^{-6}	35.97 %	0.02 %	0.05 %	0.96 %
10^{-5}	72.94 %	5.04 %	0.04 %	0.98 %
10^{-4}	85.71 %	5.61 %	0.07 %	1.95 %
10^{-3}	91.09 %	62.23 %	0.27 %	7.59 %
10^{-2}	92.70 %	212.64 %	3.17 %	22.58 %

Fig. 2. Double stub: schematic, pattern of the impedance matrix and *thresholding* effect on the solution's accuracy. S is the percentage of non-zero elements

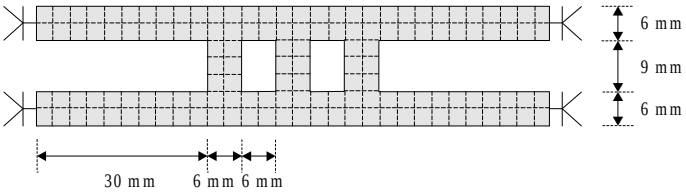

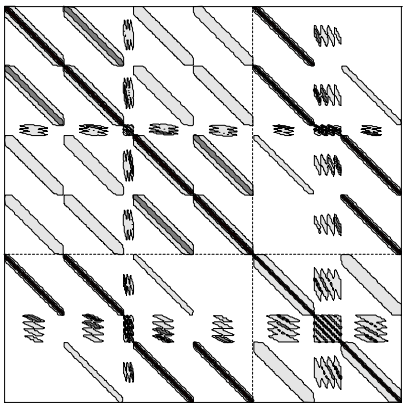

v_t	S	Solution Error	β Error	Scattering Parameter Error
10^{-7}	10.84 %	0.00 %	0.01 %	0.10 %
10^{-6}	35.41 %	0.07 %	0.04 %	0.24 %
10^{-5}	80.74 %	4.92 %	0.12 %	3.02 %
10^{-4}	93.61 %	8.14 %	0.50 %	3.83 %
10^{-3}	95.73 %	16.59 %	0.83 %	10.09 %
10^{-2}	96.55 %	143.03 %	3.71 %	34.31 %

Fig. 3. Branch coupler: schematic, pattern of the impedance matrix and *thresholding* effect on the solution's accuracy. S is the percentage of non-zero elements